Anal. Chem. **2010,** *82,* 4510–4519

Second-Order Analyte Quantitation under Identical Profiles in One Data Dimension. A Dependency-Adapted Partial Least-Squares/Residual Bilinearization Method

Valeria A. Lozano, Gabriela A. Ibañez, and Alejandro C. Olivieri*

Departamento de Química Analítica, Facultad de Ciencias Bioquímicas y Farmacéuticas, Universidad Nacional de Rosario and Instituto de Química Rosario (IQUIR-CONICET), Suipacha 531, Rosario (S2002LRK), Argentina

Analyte quantitation can be achieved from second-order data in the presence of uncalibrated components using multivariate calibration methods such as partial least-squares with residual bilinearization. However, the latter fails under conditions of identical profiles for interfering agents and calibrated components in one of the data dimensions. To overcome this problem, a new residual bilinearization procedure for linear dependency is here introduced. Simulated data show that the new model can conveniently handle the studied analytical problem, with a success comparable to multivariate curve resolution-alternating least-squares and also comparable to a version of parallel factor analysis adapted to cope with linear dependencies. The new approach has also been applied to two experimental examples involving the determination of the antibiotic ciprofloxacin in (1) urine samples from lanthanide-sensitized excitation−time decay matrixes and (2) serum samples from a novel second-order signal based on the time evolution of chemiluminescence emission. The results indicate good analytical performance of the new procedure toward the analyte in comparison with the classical approaches.

Second-order instrumental data carry the intrinsic potential of achieving the second-order advantage, which in principle permits analyte quantitation in samples containing unexpected constituents; that is, compounds not included in the calibration set.[1] Recent reviews on the subject highlight the immense potentialities of the second-order advantage in the field of complex sample analysis because it allows the training of calibration models with a limited number of standards, yet quantitating the analyte in the presence of overlapping interfering agents.[2−34]

Several algorithms are available for the convenient processing of second-order data: (1) alternating least-squares (ALS), such as parallel factor analysis (PARAFAC)[5] and its variants PARAFAC2[6] and PARALIND (PARAFAC with linear dependencies),[7] and multivariate curve resolution-ALS (MCR-ALS);[8] (2) eigenvector−eigenvalue techniques, such as generalized rank annihilation;[9] (3) direct least squares, such as bilinear least squares (BLLS);[10,11] and (4) latent-structured methods, such as unfolded partial least squares (U-PLS)[12] and multiway PLS (N-PLS).[13] All of them

* To whom correspondence should be addressed. E-mail: olivieri@iquir-conicet.gov.ar.

(1) Booksh, K. S.; Kowalski, B. R. *Anal. Chem.* **1994**, *66*, 782A–791A.
(2) Olivieri, A. C. *Anal. Chem.* **2008**, *80*, 5713–5720.
(3) Escandar, G. M.; Faber, N. M.; Goicoechea, H. C.; Muñoz de la Peña, A.; Olivieri, A. C.; Poppi, R. J. *Trends Anal. Chem.* **2007**, *26*, 752–765.
(4) Bro, R. *Crit. Rev. Anal. Chem.* **2006**, *36*, 279–293.
(5) Bro, R. *Chemom. Intell. Lab. Syst.* **1997**, *38*, 149–171.
(6) Kiers, H. A. L.; Ten Berge, J. M. F.; Bro, R. *J. Chemom.* **1999**, *13*, 275–294.
(7) Bahram, M.; Bro, R. *Anal. Chim. Acta* **2007**, *584*, 397–402.
(8) Tauler, R. *Chemom. Intell. Lab. Syst.* **1995**, *30*, 133–146.
(9) Sanchez, E.; Kowalski, B. R. *Anal. Chem.* **1986**, *58*, 496–499.
(10) Linder, M.; Sundberg, R. *Chemom. Intell. Lab. Syst.* **1998**, *42*, 159–178.
(11) Linder, M.; Sundberg, R. *J. Chemom.* **2002**, *16*, 12–27.
(12) Wold, S.; Geladi, P.; Esbensen, K.; Øhman, J. *J. Chemom.* **1987**, *1*, 41–56.
(13) Bro, R. *J. Chemom.* **1996**, *10*, 47–61.
(14) Öhman, J.; Geladi, P.; Wold, S. *J. Chemom.* **1990**, *4*, 79–90.
(15) Lozano, V. A.; Ibañez, G. A.; Olivieri, A. C. *Anal. Chim. Acta* **2008**, *610*, 186–195.
(16) Olivieri, A. C. *J. Chemom.* **2005**, *19*, 253–265.
(17) Culzoni, M. J.; Goicoechea, H. C.; Pagani, A. P.; Cabezón, M. A.; Olivieri, A. C. *Analyst* **2006**, *131*, 718–723.
(18) Prazen, B. J.; Synovec, R. E.; Kowalski, B. R. *Anal. Chem.* **1988**, *70*, 218–225.
(19) Comas, E.; Gimeno, R. A.; Ferré, J.; Marcé, R. M.; Borrull, F.; Rius, F. X. *J. Chromatogr., A* **2004**, *1035*, 195–202.
(20) Sadygov, R. G.; Maroto, F. M.; Hühmer, A. F. R. *Anal. Chem.* **2006**, *78*, 8207–8217.
(21) Skov, T.; Hoggard, J. C.; Bro, R.; Synovec, R. *J. Chromatogr., A* **2009**, *1216*, 4020–4029.
(22) Bortolato, S. A.; Arancibia, J. A.; Escandar, G. M. *Anal. Chem.* **2009**, *81*, 8074–8084.
(23) Cañada-Cañada, F.; Arancibia, J. A.; Escandar, G. M.; Ibañez, G. A.; Espinosa Mansilla, A.; Muñoz de la Peña, A.; Olivieri, A. C. *J. Chromatogr., A* **2009**, *1219*, 4868–4876.
(24) Izquierdo-Ridorsa, A.; Saurina, J.; Hernández-Cassou, S.; Tauler, R. *Chemom. Intell. Lab. Syst.* **1997**, *38*, 183–196.
(25) Espinosa-Mansilla, A.; Muñoz de la Peña, A.; Goicoechea, H. C.; Olivieri, A. C. *Appl. Spectrosc.* **2004**, *58*, 83–90.
(26) Marsili, N. R.; Lista, A.; Fernandez Band, B. S.; Goicoechea, H. C.; Olivieri, A. C. *J. Agric. Food Chem.* **2004**, *52*, 2479–2484.
(27) García-Reiriz, A.; Damiani, P. C.; Olivieri, A. C. *Talanta* **2007**, *71*, 806–815.
(28) Diewok, J.; de Juan, A.; Tauler, R.; Lendl, B. *Appl. Spectrosc.* **2002**, *56*, 40–50.
(29) Vives, M.; Gargallo, R.; Tauler, R. *Anal. Chem.* **1999**, *71*, 4328–4337.
(30) Nigam, S.; de Juan, A.; Cui, V.; Rutan, S. C. *Anal. Chem.* **1999**, *71*, 5225–5234.
(31) de Braekeleer, K.; de Juan, A.; Massart, D. L. *J. Chromatogr., A* **1999**, *832*, 67–86.
(32) Borraccetti, M. D.; Damiani, P. C.; Olivieri, A. C. *Analyst* **2009**, *134*, 1682–1691.
(33) Bohoyo Gil, D.; Muñoz de la Peña, A.; Arancibia, J. A.; Escandar, G. M.; Olivieri, A. C. *Anal. Chem.* **2006**, *78*, 8051–8058.
(34) Piccirilli, G. N.; Escandar, G. M. *Analyst* **2006**, *131*, 1012–1020.

10.1021/ac100424d
Published on Web 05/05/2010

achieve the second-order advantage, but in the case of BLLS, U-PLS, and N-PLS, this is realized only when these algorithms are combined with residual bilinearization (RBL).[14−17]

Whether the data follow a trilinear structure is of prime importance for selecting a suitable second-order multivariate algorithm for their processing. When this is the case, PARAFAC (a trilinear model itself) will adequately handle the data. However, there are circumstances in which deviations from the ideal trilinearity occur. One of these situations involves the lack of reproducibility in component profiles, which may occur from sample to sample, for example, in the presence of chromatographic retention times that vary for different experimental runs.[18−21] Different retention profiles for different samples imply a violation of the trilinearity principle (equal profiles in all samples for a given constituent).

Two options are available for processing this type of nontrilinear data sets. One of them is to restore the trilinearity by a suitable mathematical preprocessing for the alignment of retention times.[18−21] A second option is to employ a nontrilinear algorithm that is able to cope with varying component profiles among samples, such as MCR-ALS or PARAFAC2.[22] It may be noticed that the U-PLS/RBL and N-PLS/RBL methodologies should, in principle, be able to handle nontrilinear data sets; however, their application to unaligned chromatographic data remains to be checked.[23]

Another cause of trilinearity loss is the occurrence of linear dependency among component profiles due to closure relations that exist between the concentrations of conjugated acid−base species within a pH gradient or between the concentrations of reagent and product in a chemical reaction.[24] Linear dependencies cause the appearance of several minima satisfying the requirements of the trilinear model, some of which do not have physical meaning. However, the application of suitable initialization and restrictions during the least-squares PARAFAC fit may appropriately solve the problem, leading to physically reasonable solutions.[25−27] An alternative is to employ MCR-ALS[28−31] or PARALIND,[7] since both of these methods are able to cope with linear dependencies of the type mentioned above. These pH- or kinetically modulated spectral problems can also be conveniently solved by U-PLS/RBL, in this case without any algorithmic modification with respect to the regular data processing.[16,25,32] The N-PLS/RBL counterpart does not appear to be useful in this regard.[32]

Inner filter in second-order luminescence spectroscopy is ubiquitous and does also cause deviations from trilinearity because spectra are deformed in a specific manner for each chemical sample.[33] This phenomenon can be handled by MCR-ALS or PARAFAC2 only when the effect occurs on the excitation or on the emission spectra, but not when it occurs on both excitation and emission profiles. In this latter case, only U-PLS/RBL can correctly solve this interesting analytical problem.[33,34]

Finally, the existence of identical profiles for sample components, which is a special case of linear dependency, does also pose a challenge on second-order algorithms.[35] A sample with two responsive components with identical profiles in one dimension will produce a data matrix with rank one; that is, the matrix will be rank-deficient, a situation also known as *rank overlap*.[36−39] This is especially troublesome when the identical profiles correspond to a potential interfering agent and to the analyte of interest. As has been recently demonstrated, MCR-ALS and also PARALIND are the only algorithms that may be able to solve the situation.[35−41]

Table 1. Causes of Trilinearity Loss and Data Processing Alternatives

cause	trilinear algorithms	applicable nontrilinear algorithms
nonreproducibility in chromatographic or electrophoretic retention times	applicable after time alignment using suitable algorithms	MCR-ALS PARAFAC2 PLS/RBL
linear dependency in component profiles	applicable with suitable initialization and restrictions	MCR-ALS PARALIND PLS/RBL
inner filter in luminescence spectroscopy	not applicable	PLS/RBL
identical profiles for analyte and interfering agents	not applicable	MCR-ALS PARALIND

All the above causes of trilinearity losses and the corresponding solutions are summarized in Table 1. Inspection of this Table reveals an interesting fact concerning the central issue of this report: the only case that cannot be appropriately studied by U-PLS/RBL appears to be the last entry; that is, rank overlap caused by identical profiles for analyte and interfering agent. We have thus developed a new algorithm, described in detail in the corresponding section, that incorporates a modified version of the RBL procedure, which we call RBL for linear dependency (RBL-LD). The new technique is able to discriminate the analyte contribution from an interfering agent having an identical profile in one of the data dimensions and can be adequately coupled to U-PLS to yield a new, flexible second-order multivariate algorithm.

Pertinent analytical problems in which the new technique could be useful are those involving rank overlap caused by identical analyte and interfering agent profiles; for example, (1) when the kinetics of a reaction is followed and the responsive constituent is the reaction product which is unique for all sample components; (2) when the common dimension is the luminescence time decay, corresponding to a lanthanide ion whose excitation spectrum varies with the constituent that complexes the ion, and (3) when the emission spectrum of a species is common to all constituents, but the time evolution of the signal differs. We illustrate the latter two cases in the present report, corresponding to the determination of the antibiotic ciprofloxacin in serum and urine samples, respectively.

The first example has already been analyzed using MCR-ALS.[40] The latter, however, constitutes a new, second-order signal, which

(35) Culzoni, M. J.; Goicoechea, H. C.; Ibañez, G. A.; Lozano, V. A.; Marsili, N. R.; Olivieri, A. C.; Pagani, A. P. *Anal. Chim. Acta* **2008**, *614*, 46–57.
(36) Smilde, A. K.; Wang, Y.; Kowalski, B. R. *J. Chemom.* **1994**, *8*, 21–36.
(37) Izquierdo-Ridorsa, A.; Saurina, J.; Hernández-Cassou, S.; Tauler, R. *Chemom. Intell. Lab. Syst.* **1997**, *38*, 183–196.
(38) Saurina, J.; Hernández-Cassou, S.; Tauler, R.; Izquierdo-Ridorsa, A. *J. Chemom.* **1998**, *12*, 183–203.
(39) Smilde, A. K.; Tauler, R.; Saurina, J.; Bro, R. *Anal. Chim. Acta* **1999**, *398*, 237–251.
(40) Lozano, V. A.; Tauler, R.; Ibañez, G. A.; Olivieri, A. C. *Talanta* **2009**, *77*, 1715–1723.
(41) Vera-Candioti, L.; Culzoni, M. J.; Olivieri, A. C.; Goicoechea, H. C. *Electrophoresis* **2008**, *29*, 4527–4537.

comprises as one of the data dimensions the time evolution of the chemiluminescent signal of a ruthenium complex, which depends on the complex ion structure and, thus, on the chemical component forming this complex. The second dimension, in turn, is common to all constituents: the ruthenium chemiluminescent emission spectrum. It is interesting to note that in both of the experimental cases analyzed in the present report, calibration had to be made in the standard addition mode, which is a relatively unexplored second-order calibration field.[40,42] The literature on chemiluminescent analysis of fluoroquinolones has been recently reviewed.[43] Although several works have been performed on pharmaceutical and biomedical analysis,[44−47] none of them employed second-order signals, such as those presently discussed.

EXPERIMENTAL SECTION

Instrumentation and Software. For the experimental system 1, an SLM Aminco Bowman Series 2 luminescence spectrometer was used, collecting data matrices using excitation wavelengths every 5 nm from 240 to 350 nm (23 data points), and decay times every 25 μs from 225 to 800 μs (24 data points). For further details see ref 40.

For the experimental system 2, chemiluminescence emission measurements as a function of time were made on a Varian Cary Eclypse (Varian, Mulgrave, Australia) spectroluminometer equipped with a 7 W xenon lamp, connected to a PC microcomputer, using 1.00 cm quartz cells. Instrumental parameters were emission slit, 10 nm; emission wavelength, 550−650 nm (every 5 nm); time cycles, 0.0 to 13.92 s (every 0.48 s); photomultiplier voltage, 800; and scan rate, 24 000 nm min^{-1}. All measurements were made at 20 °C.

Data were saved in ASCII format and transferred to a PC Sempron AMD microcomputer for subsequent manipulation by the multivariate programs.

Reagents. All chemicals used were of analytical reagent grade. For the experimental system 1, see ref 40. For the experimental system 2, the following solutions were employed: ciprofloxacin, 1000 mg L^{-1} (Fluka, Sigma-Aldrich, Steinheim, Germany), prepared in 0.01 mol L^{-1} sulphuric acid (Merck, Darmstadt, Germany); cerium(IV), 6.00×10^{-2} mol L^{-1}, prepared from cerium(IV) sulfate tetrahydrate (Merck, Darmstadt, Germany) and dissolved in sulphuric acid, 10 mol L^{-1}; tris(2,2′-bipyridil)-dichlororuthenium(II) hexahydrate [$Ru(bipy)_3^{2+}$], 4.00×10^{-3} mol L^{-1} (Sigma-Aldrich, St. Louis, MO), prepared by dissolving the required amount in doubly distilled water. Working solutions of different concentrations were prepared by dilution of the stock solutions with distilled water.

Analytical Protocol. For the experimental system 1, 16 serum samples spiked with the analyte and with the interfering agent salycilate were prepared. To each of these samples, three standard additions of the analyte ciprofloxacin were carried out. See additional details in ref 40.

For the experimental system 2, 14 different spiked urine samples were prepared from 7 different urines taken from healthy individuals. Appropriate aliquots of the corresponding stock solution of ciprofloxacin; 200 μL of urine; 400 μL of [$Ru(bipy)_3^{2+}$]; and 500 μL of sulphuric acid, 2.0 mol L^{-1}, were placed in a 2.00 mL volumetric flask and completion to the mark was achieved with distilled water. The solution was placed in the measuring cell, and the sample was homogenized with a magnetic stirrer. After 300 μL of Ce(IV) was manually injected into the cell by a syringe, the chemiluminescence signal was measured immediately. Three additional samples were prepared in an analogous manner, except that an analyte stock solution (10.0 μL) was added in such a way that the analyte concentrations were increased by 5.00, 10.0, and 15.0 mg L^{-1}, respectively. After each addition, the samples were homogenized. The final concentrations for the analyzed drug were from 0.00 to 33.0 mg L^{-1} (values refer to the measuring cell). The degree of urine dilution (1:10) was such that the maximum urine concentration of the studied drug was 180 mg L^{-1}. The concentration range is within the therapeutic values of the studied drug in human urine.

THEORY

The MCR-ALS Model. This algorithm has recently been shown to be capable of coping with the problem of identical profiles for sample components by resorting to matrix augmentation in the affected dimension.[35] For details, refer to the latter work. In the present report, we have employed a recently introduced version of MCR-ALS, which includes a so-called concentration correlation constraint, incorporating a regression of MCR scores against the nominal analyte concentration within the least-squares fitting phase.[48−50] This version is more suitable for quantitative analytical purposes, since it provides the model with concentration information during the matrix decomposition phase of the algorithm.

The PARALIND Model. A modification of PARAFAC taking into account linear dependencies among component profiles involves the decomposition of a three-way data array into four matrices instead of three. The following is the model equation for a single data matrix, **X** (size $J \times K$, where J and K are the number of instrumental channels in the first and data dimensions):

$$\mathbf{X} = \mathbf{BYHC}^{\mathrm{T}} + \mathbf{E} \qquad (1)$$

where the four output data matrices are (1) **B**, a matrix of loadings in the first data dimension (size $J \times N$, where N is the total number of responsive components); (2) **H**, a matrix that incorporates the linear dependency in the model (size $N \times M$, where M is the number of unique profiles in the second dimension); (3) **Y**, a diagonal matrix of sample scores, collecting in the diagonal the relative concentrations of all components in the sample (size $N \times N$); and (4) **C**, a matrix of unique loadings in the second data dimension (size $K \times M$). The matrix **E** contains the model errors. The diagonals of the **Y** matrices for all samples are then collected into the score **A** matrix (size $I \times N$, where I is the number of

(42) Lozano, V. A.; Ibañez, G. A.; Olivieri, A. C. *Anal. Chim. Acta* **2009**, *651*, 165–172.
(43) Francis, P. S.; Adcock, J. L. *Anal. Chim. Acta* **2005**, *541*, 3–12.
(44) Murillo, J. A.; Alañón Molina, A.; Muñoz de la Peña, A.; Durán Merás, I.; Jiménez Girón, A. *J. Fluoresc.* **2007**, *17*, 481–491.
(45) Sun, H.-W.; Li, L.-Q.; Chen, X.-Y.; Shi, H.-M.; Lü, Y.-K. *Can. J. Anal. Sci. Spectrosc.* **2006**, *51*, 100–107.
(46) Li, Y.; Lu, J. *Anal. Chim. Acta* **2006**, *577*, 107–110.
(47) Zhuoyong, Z.; Xia, L.; Xiaoli, W.; Shilu, C.; Baohua, S.; Huichun, Z. *J. Rare Earths* **2006**, *24*, 285–288.
(48) Antunes, M. C.; Simao, J. E. J.; Duarte, A. C.; Tauler, R. *Analyst* **2002**, *127*, 809–817.
(49) Azzouz, T.; Tauler, R. *Talanta* **2008**, *74*, 1201–1210.
(50) Goicoechea, H. C.; Olivieri, A. C.; Tauler, R. *Analyst* **2010**, *135*, 636–642.

samples). In the presently studied simulated and experimental examples, where two components occur, having identical profiles in the second data dimension but different profiles in the first one, **B** contains two columns (corresponding to each of the distinguishable component profiles in dimension one), but **C** contains only a single profile (the common profile to both components in the second dimension). The matrix **H** is initially given the following form:

$$\mathbf{H} = \begin{bmatrix} 1 \\ 1 \end{bmatrix} \tag{2}$$

which causes the matrix product ($\mathbf{H} \times \mathbf{C}^{\mathrm{T}}$) to have two identical loadings in the second data dimension or K dimension (see eq 1). During the PARALIND fit, nonnegativity restrictions were imposed on the elements of all output matrices to retrieve scores and loadings having physical meaning. Initialization of PARALIND can be made using known scores and loadings or adequately dimensioned matrices containing random numbers. We have employed this latter option, which makes the algorithm more automatic in its operation.

It should be noticed in this context that the MCR-ALS algorithm has also been employed using interaction constraints, with a different number of components in different modes; for example, in the study of the geographical distributions of metals in fish, sediments, and river waters.[51] Similar situations have been faced by constrained Tucker3 models, which were applied to both quantitative and qualitative studies.[52]

The U-PLS/RBL Model. U-PLS first unfolds the calibration second-order data into vectors.[12] Analyte concentration information is then employed to calibrate a model without including data for the unknown sample. With the I_{cal} calibration data matrices, all vectorized into $JK \times 1$ vectors, and the vector of calibration concentrations, **y** (size $I_{\mathrm{cal}} \times 1$), a usual PLS model is built. This provides a set of loadings, **P**, and weight loadings, **W** (both of size $JK \times A$, where A is the number of latent factors), as well as regression coefficients, v (size $A \times 1$), with the parameter A usually selected by leave-one-out cross-validation.[53]

If no unexpected components occurred in the test sample, **v** could be employed to estimate the analyte concentration according to

$$y_{\mathrm{u}} = t_{\mathrm{u}}^{\mathrm{T}} v \tag{3}$$

where t_{u} is the test sample score obtained by projecting the vectorized data for the test sample, $\mathrm{vec}(\mathbf{X}_{\mathrm{u}})$, onto the space of the A latent factors:

$$t_{\mathrm{u}} = (\mathbf{W}^{\mathrm{T}}\mathbf{P})^{-1}\mathbf{W}^{\mathrm{T}}\,\mathrm{vec}(\mathbf{X}_{\mathrm{u}}) \tag{4}$$

where $\mathrm{vec}(\cdot)$ is the vectorization operator.

When unexpected constituents occur in $\mathbf{X}_{\mathrm{u}}$, the sample scores given by eq 4 are unsuitable for analyte prediction through eq 3. In this case, the residuals of the U-PLS prediction step [s_{p}, see eq 5 below] will be abnormally large in comparison with the instrumental noise level:

$$\begin{aligned} s_{\mathrm{p}} &= \|\mathbf{e}_{\mathrm{p}}\|/(JK - A)^{1/2} = \|\mathrm{vec}(\mathbf{X}_{\mathrm{u}}) - \\ &\quad \mathbf{P}(\mathbf{W}^{\mathrm{T}}\mathbf{P})^{-1}\mathbf{W}^{\mathrm{T}}\,\mathrm{vec}(\mathbf{X}_{\mathrm{u}})\|/(JK - A)^{1/2} \\ &= \|\mathrm{vec}(\mathbf{X}_{\mathrm{u}}) - \mathbf{P}\mathbf{t}_{\mathrm{u}}\|/(JK - A)^{1/2} \end{aligned} \tag{5}$$

where $\|\cdot\|$ indicates the Euclidean norm.

In general, this new situation can be handled by residual bilinearization on the basis of principal component analysis (PCA) to model the unexpected effects.[14,16] However, this classical RBL procedure is not appropriate when the unexpected components have profiles that are identical to the analyte profile in one of the data dimensions.[35]

We now propose a new RBL procedure for linear dependency (RBL-LD). The underlying idea is similar to that of the classical RBL method: to minimize the norm of the residual vector $\mathbf{e}_{\mathrm{u}}$, computed by fitting the test data to the sum of the relevant contributions (i.e., the part that is modeled by the current calibration and the contribution from the interfering agents) but taking into account the identical profiles in one of the data dimensions. This can be done either by modeling the residuals with MCR-ALS or with PARALIND, as discussed in the following two sections.

The RBL-LD Model Using MCR-ALS. One alternative to model the contribution of the interfering agent is to employ MCR-ALS, formally expressed as in the following equation:

$$\mathrm{vec}(\mathbf{X}_{\mathrm{u}}) = \mathbf{P}\mathrm{t}_{\mathrm{u}} + \mathrm{vec}[\mathbf{S}_{\mathrm{unx}}(\mathbf{C}_{\mathrm{unx}})^{\mathrm{T}}] + \mathbf{e}_{\mathrm{u}} \tag{6}$$

Unlike the PCA-based RBL procedure, the new RBL-LD method models the interfering agent signal by the product of matrices $\mathbf{S}_{\mathrm{unx}}$ and $\mathbf{C}_{\mathrm{unx}}$ containing the interfering agent spectral and concentration profiles, respectively. They are retrieved by MCR-ALS analysis on an augmented data matrix **D** [size $J \times (1 + I_{\mathrm{cal}})K$], constructed by augmenting a residual data matrix with the I_{cal} calibration matrices $\mathbf{X}_{\mathrm{cal},i}$:

$$\mathbf{D} = [\mathbf{E}_{\mathrm{p}}|\mathbf{X}_{\mathrm{cal},1}||\mathbf{X}_{\mathrm{cal},2}|\cdots|\mathbf{X}_{\mathrm{cal},I_{\mathrm{cal}}}] \tag{7}$$

where $\mathbf{E}_{\mathrm{p}}$ is the residual $J \times K$ matrix obtained after reshaping the $JK \times 1$ $\mathbf{e}_{\mathrm{p}}$ residual vector of eq 5. The direction of matrix augmentation, assumed to correspond to the K channels, is selected as the one for the identical component profiles.

The MCR-ALS decomposition of matrix **D** is then carried out by the following least-squares model:

$$\mathbf{D} = \mathbf{S}_{\mathrm{unx}}\mathbf{G}_{\mathrm{unx}}^{\mathrm{T}} + \mathbf{E}_{\mathrm{MCR}} \tag{8}$$

where $\mathbf{S}_{\mathrm{unx}}$ and $\mathbf{G}_{\mathrm{unx}}$ contain the profiles [size $J \times (A + N_{\mathrm{RBL\text{-}LD}})$ and $K(1 + I_{\mathrm{cal}}) \times (A + N_{\mathrm{RBL\text{-}LD}})$, respectively, where $N_{\mathrm{RBL\text{-}LD}}$ is the number of interfering components]. The matrix $\mathbf{E}_{\mathrm{MCR}}$ collects the errors not fitted by the MCR model. Notice that the matrix $\mathbf{G}_{\mathrm{unx}}$ contains $(1 + I_{\mathrm{cal}})$ successive component profiles, each of size $K \times (A + N_{\mathrm{RBL\text{-}LD}})$. The first submatrix of $\mathbf{G}_{\mathrm{unx}}$ corresponds to the profiles in matrix $\mathbf{E}_{\mathrm{p}}$, and the remaining ones, to those in the successive calibration matrices:

(51) Peré-Trepat, E.; Ginebreda, A.; Tauler, R. *Chemom. Intell. Lab. Syst.* **2007**, *88*, 69–83.
(52) Kiers, H. A. L.; Smilde, A. K. *J. Chemom.* **1998**, *12*, 125–147.
(53) Haaland, D. M.; Thomas, E. V. *Anal. Chem.* **1988**, *60*, 1193–1202.

$$\mathbf{G}_{unx} = \begin{bmatrix} \mathbf{C}_{unx} \\ \mathbf{C}_{cal,1} \\ \mathbf{C}_{cal,2} \\ \cdots \\ \mathbf{C}_{cal,I_{cal}} \end{bmatrix} \quad (9)$$

It is clear that to estimate the required contribution of the unexpected components in eq 6, only the submatrix $\mathbf{C}_{unx}$ is needed, in which the concentration profiles corresponding to the analytes are set to zero, thanks to the species correspondence (see below). It is thus irrelevant whether these analyte profiles are left in $\mathbf{C}_{unx}$ when inserted into eq 6.

The MCR-ALS model of eq 8 can be initialized using an estimation of either the spectral or concentration profiles for each intervening species. Different methods can be used for this purpose, such as evolving factor analysis[54] or the determination of the purest variables,[55−57] depending on the data structure. These procedures may provide initial spectra or concentrations. In our case, it was found that the estimation of pure variables in the concentration mode was preferable.

During the fitting of eq 8, constraints can be applied, such as nonnegativity, unimodality, closure, etc., which are regularly employed in MCR-ALS studies. They help to improve the solutions, to give them physical meaning, and to limit their possible number for the same data fitting.[58] Iterations continue until an optimal solution is obtained that fulfills the postulated constraints and the established convergence criterion. Nonnegativity constraints are applied to the concentration profiles due to the fact that the concentrations of the chemical species are always either positive values or zero. In our case, nonnegativity constraints are also applied for spectra. Unimodality and closure, respectively, can be applied to profiles having a single maximum and to fulfill chemical mass balance equations among different chemical species in equilibrium or in kinetics. Finally, the correspondence among species and data matrices can also be established because the model can be restricted so that the analyte is absent in the residual $\mathbf{E}_p$ matrix and the interfering agent is absent in the calibration matrices.

During the RBL-LD procedure applied to eq 6, $\mathbf{P}$ is kept constant at the calibration values, and $\mathbf{t}_u$ is varied until $||\mathbf{e}_u||$ is minimized using a Gauss−Newton procedure. Once $||\mathbf{e}_u||$ is minimized, the analyte concentrations are provided by eq 3 by introducing the final $\mathbf{t}_u$ vector found by the RBL-LD procedure. The complete process is outlined in Figure 1.

When a single interfering agent occurs, the RBL-LD analysis provides real interfering agent profiles in both data dimensions. For additional, unexpected constituents, however, the retrieved profiles may not resemble true spectra. For example, if two or more interfering agents occur that have the same profile in one of the data dimensions, they will be interpreted as a single component, and the retrieved profiles in that specific dimension will be composed of linear combinations instead of by pure component spectra.

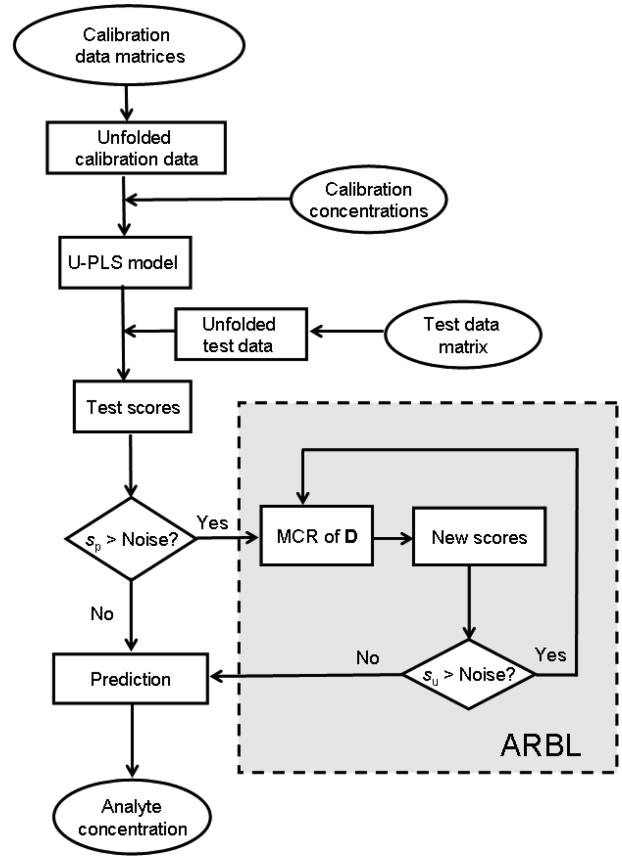

Figure 1. Scheme illustrating how the new U-PLS/RBL-LD method works. See text for explanation of symbols.

We notice that the aim that guides the RBL-LD procedure is the minimization of the residual error s_u to a level compatible with the degree of noise present in the measured signals, with s_u given by[59]

$$s_u = ||\mathbf{e}_u||/[(J - N_{RBL\text{-}LD})(K - N_{RBL\text{-}LD}) - A]^{1/2} \quad (10)$$

Therefore, if more than one unexpected component is considered, RBL-LD should select the simplest model giving a residual value that is not statistically different from the minimum one.[59]

It should be noted that the presently described U-PLS/RBL-LD procedure is completely general, in the sense that it can also be applied to cases in which selectivity is achieved in both data dimensions. What is unique to this new model, however, is the case in which selectivity is lost in one of the data dimensions, particularly between analyte and interferences, a case that is clearly not covered by the classical RBL method.

The RBL-LD Model Using PARALIND. A second alternative to RBL-LD is to model the interfering agent's contribution with PARALIND. In this case, instead of constructing an augmented matrix, a three-way array is built with the residual matrix $\mathbf{E}_p$ and the calibration matrices. This array is decomposed using PARALIND, as described in the corresponding section, and then selecting the loadings and scores for the interfering agent to be included in the RBL model,

$$\mathrm{vec}(\mathbf{X}_u) = \mathbf{P}\mathbf{t}_u + \mathrm{vec}[\mathbf{B}_{unx}\mathbf{Y}_{unx}\mathbf{H}_{unx}(\mathbf{C}_{unx})^T] + \mathbf{e}_u \quad (11)$$

(54) Maeder, M. *Anal. Chem.* **1987**, *59*, 527–530.
(55) Windig, W.; Guilment, J. *Anal. Chem.* **1991**, *63*, 1425–1432.
(56) Windig, W.; Stephenson, D. A. *Anal. Chem.* **1992**, *64*, 2735–2742.
(57) Windig, W.; Heckler, C. E. *Chemom. Intell. Lab. Syst.* **1992**, *14*, 195–207.
(58) Tauler, R.; Smilde, A.; Kowalski, B. R. *J. Chemom.* **1995**, *9*, 31–58.
(59) Bortolato, S.; Arancibia, J. A.; Escandar, G. M. *Anal. Chem.* **2008**, *80*, 8276–8286.

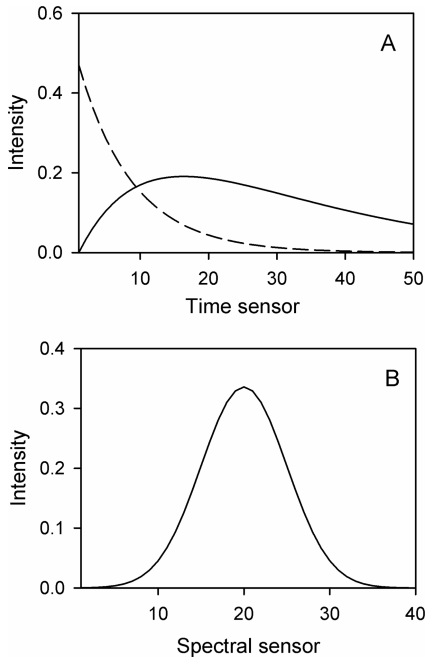

Figure 2. Noiseless profiles employed for the simulations in the time (A) and spectral dimension (B). In both cases, the solid line corresponds to the analyte; the dashed line, to the potential interfering agent. All profiles are normalized to unit length.

where $\mathbf{B}_{unx}$, $\mathbf{Y}_{unx}$, $\mathbf{H}_{unx}$, and $\mathbf{C}_{unx}$ have the same meaning as in eq 1, but contain only information regarding the interfering agents in the test sample.

As before, during the application of this model, the calibration $\mathbf{P}$ matrix is kept constant, and $\mathbf{t}_u$ varies to minimize $||\mathbf{e}_u||$. Analyte quantitation then proceeds via eq 3.

Simulations. To illustrate the behavior of the new second-order calibration algorithm U-PLS/RBL-LD and to compare its performance with other algorithms, simulations were carried out. In the simulated system, a single analyte was considered to be present in the calibration samples, whereas the latter component and also an additional one were included in the test samples. Thus, proper resolution of this system requires adherence to the second-order advantage. Time−spectral matrix data were generated starting from noiseless spectral and time profiles that are shown in Figure 2A and B, respectively. As can be seen, both components have identical spectra, but differ in their time profiles. From the profiles shown in Figure 2, a calibration set of four matrices was built containing only the analyte at nominal concentrations of 0.25, 0.50, 0.75, and 1.00 (in arbitrary units). The size of each of these matrices was 50 × 40 (50 data points correspond to the time dimension, and 40, to the spectral dimension, where the spectra are identical). A set of 100 test samples having random concentrations of the analyte in the range 0−1 and of the interfering agent in the range 0.5−1.5 (to ensure that all test samples contained significant amounts of the interfering agent) was also created. To all of these second-order signals, noise was added from a Gaussian distribution having a standard deviation equal to 1% of the maximum calibration signal.

With respect to the analyte calibration and test concentrations, the nominal values employed for building the calibration and test spectra were not directly employed for calibrating the model for analyte quantitation and for comparing the model predictions with the nominal values respectively. Instead, and to mimic a real analytical experiment in which the sample preparation always carries some degree of uncertainty in the final analyte concentrations, Gaussian-distributed noise with a standard deviation of 0.01 unit was added to all nominal concentrations. The final values were employed for calibration and for comparison of that predicted with nominal analyte concentrations in the test samples. This intends to resemble the existence of an average error of 0.01 concentration units in the analyte concentration during the preparation of all samples. Since the maximum concentration is 1 unit, then the concentration uncertainty level introduced in these simulations is also 1%, analogous to that employed in the case of the signal noise (see above).

The second-order data for each of the 100 test samples were then joined to those for the calibration set, and each five-sample data set was submitted to second-order calibration with PARAFAC, U-PLS/RBL, PARALIND, MCR-ALS, and both versions of the novel U-PLS/RBL-LD. Specific analyte predictions were stored for statistical analysis and future comparison.

Software. All calculations were carried out using MATLAB 7.0.[60] The PARAFAC and PARALIND programs are available thanks to Bro in the Internet at www.models.kvl.dk/source/.[5] MCR-ALS was implemented using the concentration correlation constraint developed by R. Tauler.[48−50] The routines for performing U-PLS/RBL are available on the Internet at http://www.chemometry.com/Index/Links%20and%20downloads/Programs.html.[61] All simulations and the new U-PLS/RBL-LD method were implemented using in-house routines.

RESULTS AND DISCUSSION

Simulations. In the simulated system, the time profiles for the calibrated analyte and the interfering agent differ, but the spectra are identical (Figure 2). These profiles resemble those to be encountered in the experimental system 2, in which the time evolution of the signal is different for each sample component, but the emission spectra are identical. In the simulated system, the analyte is present only in the calibration set, but all test samples contain both constituents, an analytical situation which requires the second-order advantage for accurate analyte quantitation. Notice that data processing using all algorithms was performed under the previously known fact that the system involves two components: one calibrated analyte and one interfering agent. In a real case, however, these numbers must be established using suitable statistical analysis of the available experimental data, as will be explained below.

When PARAFAC and U-PLS/RBL were applied in the usual manner to determine the analyte in the 100 test sample data set of this simulated system, poor recoveries were obtained. The results are shown in Figure 3 in the form of a box-and-whisker plot for convenient comparison with the remaining algorithms.

As previously discussed, MCR-ALS can be applied to this problem in the spectral augmentation mode. In this way, the linear dependency of the spectral profiles between analyte and interfering agent is conveniently broken, since the interfering agent occurs only in the test matrix, and hence, its augmented spectral

(60) *MATLAB 7.0*; The Mathworks: Natick, MA, 2003.
(61) Olivieri, A. C.; Wu, H.-L.; Yu, R.-Q. *Chemom. Intell. Lab. Syst.* **2009**, *96*, 246–251.

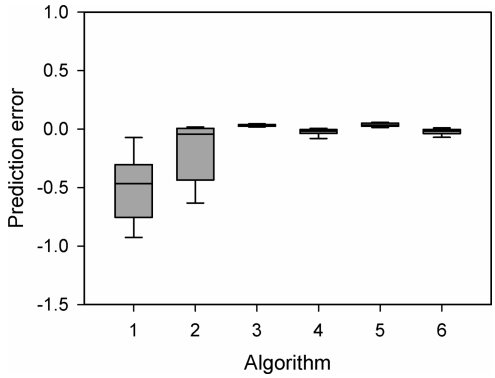

Figure 3. Box-and-whisker plot of the 100 prediction results corresponding to the simulated study. Algorithms are numbered in the horizontal axis as follows: (1) U-PLS/RBL, (2) PARAFAC, (3) MCR-ALS, (4) PARALIND, (5) U-PLS/RBL-LD (MCR version), and (6) U-PLS/RBL-LD (PARALIND version). For each algorithm, the gray boxes are bounded by the 25% and 75% quartiles with the median inside, whereas the extreme levels correspond to 5% and 95% quartiles.

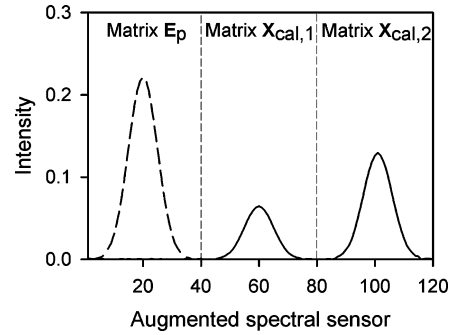

Figure 4. Profiles retrieved on applying U-PLS/RBL-LD to a typical test simulated sample in the augmented spectral dimension. Only the residual submatrix, $\mathbf{E}_p$, and the first two calibration matrices are shown, as indicated. The solid line corresponds to the analyte, and the dashed line, to the potential interfering agent. The augmented profiles show the relative contribution of the analyte in the calibration samples and the contribution of the interfering agent with respect to the analyte in this particular test sample.

profile differs from that for the analyte, which in principle is present in all samples. An augmented data matrix was created with each test sample and the calibration data matrices in such a way that the augmented matrix was of size 50×200 (corresponding to placing five matrices adjacent to each other in the spectral dimension; one of them was the test data matrix, and the remaining four, the calibration data matrices). Decomposition was then performed by imposing the restriction of nonnegativity for both component profiles in both dimensions. Another constraint imposed on the model during ALS minimization was the correspondence among species; that is, information was supplied on the absence of the interfering agent in all calibration samples. Finally, the concentration constraint was also applied, which correlates the nominal analyte concentration in the calibration samples with the corresponding scores during the alternating least-squares fitting phase. The results (Figure 3) show good agreement between nominal and predicted concentration values.

Similarly, the PARALIND model was applied to the set of simulated 100 test samples, as described above. In this case, the introduction of an interaction matrix **H** in the model eq 1 allows one to decompose the three-way data formed by each sample data matrix and the four calibration matrices in terms of a single spectral loading and two time dimension loadings. The scores contained in the **A** matrix were then converted to predicted analyte concentrations by a usual pseudounivariate calibration plot. The results are shown in Figure 3, and point to good predictive ability of this model regarding the simulated data set.

Finally, the new U-PLS/RBL-LD model was applied to the simulated data set. In this case, calibration was performed using a single latent variable for building the U-PLS model (i.e., $A = 1$), and a single RBL-LD component was considered in modeling the contribution from the interfering agent (i.e., $N_{\text{RBL-LD}} = 1$). For implementing the RBL-LD procedure, MCR-ALS and PARALIND were separately employed. In the MCR-ALS version, the residual matrix, $\mathbf{E}_p$, was augmented with the calibration data matrices, with augmentation in the spectral direction.

It is worth discussing the profiles retrieved by the RBL-LD procedure, since the success of this activity is crucial to the achievement of the second-order advantage for this model. Figure 4 shows the profiles retrieved in the spectral dimension during the analysis of a typical test sample. As can be seen, correct augmented spectra are recovered, with the expected behavior in terms of the absence and presence of a given component in each of the samples analyzed by the RBL-LD methodology, as indicated in Figure 4.

When applying the PARALIND version of RBL-LD, the residual matrix and the calibration matrices were joined into a single three-way array. The profiles recovered by decomposition of this array were similar to those presented in Figure 2, which were used to build the simulated data.

The specific prediction results (Figure 3) are similar to MCR-ALS and PARALIND. In establishing a comparison among these algorithms, the statistical results lead to the following (average) biases and root-mean-square error (RMSE) values: MCR-ALS, 0.033 and 0.032; PARALIND, 0.034 and 0.055; U-PLS/RBL-LD (MCR-ALS), 0.034 and 0.034; and U-PLS/RBL-LD (PARALIND), 0.030 and 0.040 (all results are expressed in arbitrary concentration units). These figures indicate comparable biases among all the methodologies, but slightly better RMSE values both for MCR-ALS and of U-PLS/RBL-LD in the MCR-ALS version.

Experimental System 1. This system has already been analyzed using MCR-ALS.[40] In the present case, we compare the performance of this latter algorithm with that of PARALIND and with the two versions of the new U-PLS/RBL-LD algorithm herein introduced. The first issue to be noticed is that calibration was done in the standard addition mode due to the changes suffered by the second-order signal of the analyte in the presence of the serum background.[40] To improve the analytical results, a modified version of standard addition was applied in which the test data matrix is digitally subtracted from the standard addition data matrices, creating a new set of calibration matrices that is analogous to the external calibration philosophy. However, the analyte suffers the same interactions and spectral modifications in these virtual calibration samples as in the test sample itself.[42] Interestingly, this methodology allowed us to employ the U-PLS/RBL model in the standard addition version, as described in detail in ref 42. We have employed a similar philosophy in the present

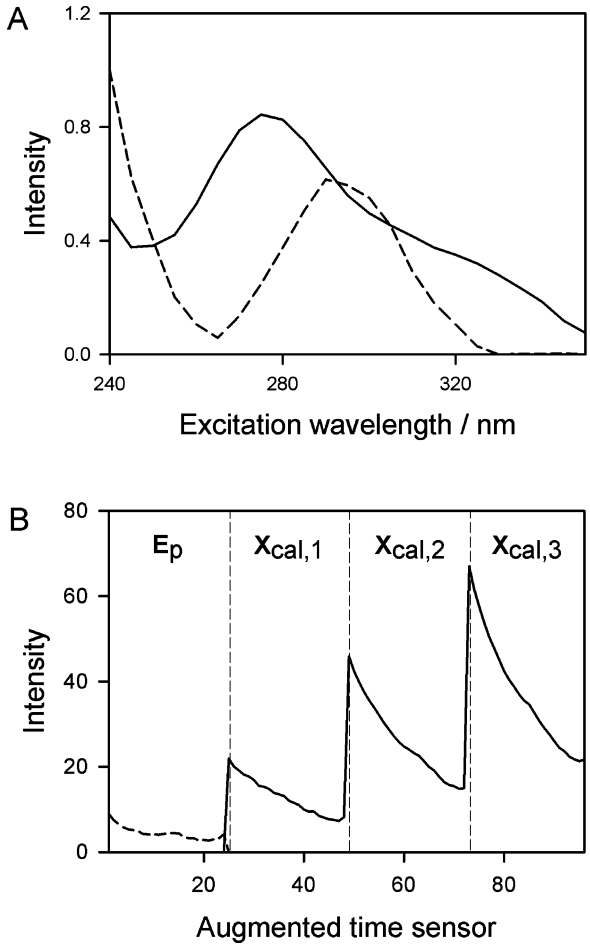

Figure 5. Profiles retrieved by U-PLS/RBL-LD (MCR-ALS version) during analysis of a typical serum sample containing ciprofloxacin and salycilate: (A) excitation profiles and (B) augmented time decay profiles. In both cases, the solid lines correspond to the analyte, and the dashed lines, to the interfering agent. The residual submatrix, $\mathbf{E}_p$, and the virtual calibration matrices are indicated. Vertical intensities are in arbitrary units.

work, which allowed us to apply the novel U-PLS/RBL-LD combined algorithm in the standard addition mode.

We briefly describe the results obtained with U-PLS/RBL-LD in the MCR-ALS version, which according to simulations appears to be the most successful one. Before specific sample analysis, the number of calibration U-PLS latent variables must be assessed. Leave-one-out cross-validation allowed us to set this number as 1. During a typical analysis of a spiked serum sample of the experimental system 1, the number of RBL-LD components was estimated by computing the final residue s_u (eq 10) for increasing trial numbers of interfering agents. This analysis led to the conclusion that s_u stabilizes at a single RBL-LD component.

Component profiles were then retrieved in the excitation and in the (augmented) time decay dimensions, as shown in Figure 5A and B, respectively. The latter are the expected profiles for analyte and interfering agent, as can be confirmed by comparison of Figure 5 with Figure 6 of ref 40. Moreover, the contributions from the analyte and interfering agent are clearly separated, as observed in Figure 5B: the interfering agent is present only in the residual matrix, $\mathbf{E}_p$, whereas the analyte is present in the virtual calibration matrices, as indicated in Figure 5. Therefore, in terms of profile retrieval, U-PLS/RBL-LD appears to be as successful as MCR-ALS for these spectroscopic systems, an essential property that is required to achieve the important second-order advantage.

Table 2. Prediction of Ciprofloxacin in Serum Samples by Several Second-Order Models from Excitation−Time Decay Sensitized Lanthanide Luminescence Data[a]

	ciprofloxacin				
				U-PLS/RBL-LD	
serum	nominal	MCR-ALS	PARALIND	MCR-ALS[b]	PARALIND[b]
A	4.4	4.8	4.3	4.6	4.7
D	4.4	3.8	2.4	3.6	3.5
A	4.8	4.6	4.0	4.4	4.2
A	3.8	3.8	3.0	3.6	3.5
B	2.8	3.2	2.6	3.2	3.3
B	0.0	0.4	0.0	0.4	0.4
B	2.6	2.4	2.0	2.4	2.2
D	2.6	3.0	2.4	3.0	3.0
C	3.4	3.4	4.2	3.2	3.0
D	3.4	4.0	6.0	4.0	4.1
C	3.4	2.8	3.4	2.8	2.6
C	3.6	3.0	4.4	3.2	3.2
D	3.6	3.8	5.0	3.8	3.9
E	1.6	1.6	2.0	1.4	1.2
E	1.6	2.0	2.0	1.8	1.7
F	1.6	2.0	3.4	2.0	2.1
	RMSE[c]	0.4	1.1	0.4	0.5
	REP[d]	13	37	13	17

[a] All concentrations are in milligrams per liter, referred to the original serum samples. Concentrations in the measuring cell are 20 times smaller. All samples contain salicylate in concentrations varying from 4.00 to 11.80 mg L^{-1}. The letters identify the different sera employed. [b] The specific version in which the RBL-LD procedure is indicated. [c] RMSE = root-mean-square error in milligrams per liter. [d] REP = relative error of prediction in percent.

More important, however, are the specific prediction results that are collected in Table 2, in terms of predicted concentrations referred to the original serum samples. As can be seen, the predictive quality of the new model is comparable to that of MCR-ALS, achieving an analogous RMSE value of 0.4 mg L^{-1}, satisfactory in view of the complexity of the analyzed samples and the challenges to the different algorithms posed by the data structure. The relative error of prediction (REP) associated with this RMSE value is 13%, computed with respect to the mean of the nominal analyte concentrations.

Further insight into the accuracy of the method can be gathered from the basis of paired *t*-statistics.[62] Specifically, the differences (Δ) between nominal and predicted concentrations are first computed for the U-PLS/RBL-LD method. Paired *t*-statistics compares the experimental t_{exp} with the critical t_{crit}, where $t_{exp} = |\bar{\Delta}|(n-1)^{1/2}/s$ ($\bar{\Delta}$ and s are the mean and standard deviation of the different Δ values; n, the number of pairs; and $||$ indicates modulus). Since $t_{exp} = 0.11$, lower than $t_{crit} = 2.13$ (95% confidence level and 15 degrees of freedom), the results provided by U-PLS/RBL-LD are statistically comparable to the nominal ones. A recovery test was also applied to these prediction results:[63] the mean recovery, $\bar{R}$, computed for the test samples (except the blank sample no. 6 in Table 2) was 100.6%. This leads to a value of $t_{exp} = |\bar{R} - 100|(n-1)^{1/2}/s_R$ (s_R

(62) Miller, J. N.; Miller, J. C. *Statistics and Chemometrics for Analytical Chemistry*; Pearson-Prentice Hall: New York, 2005; Chapter 2.

(63) González, A. G.; Herrador, M. A.; Asuero, A. G. *Talanta* **1999**, *48*, 729–736.

is the standard deviation for the recoveries). In this way, $t_{exp} = 0.15$, again lower than t_{crit} (2.15 for 14 degrees of freedom), confirming that the mean recovery is statistically indistinguishable from 100%.

It should be noted that application of PARALIND and U-PLS/RBL-LD in the alternative PARALIND version rendered poorer results for this analyte in this particular group of samples. This result is similar to that obtained for the simulations, although it is difficult to predict if this is a general phenomenon.

Experimental System 2. In the new experimental system 2, chemiluminescence has been measured as a function of evolution time for a ruthenium complex of the analyte ciprofloxacin in the interfering background of human urine samples. Ruthenium chemiluminescence has proven to be a very sensitive detection system for compounds bearing a secondary or tertiary aliphatic amine, such as the presently studied analyte.[64] A mechanism for chemiluminescence emission involving the oxidation of the complex $Ru(bipy)_3^{2+}$ and the amine has been proposed.[65] The amine oxidation product decomposes to form a radical, which reduces $Ru(bipy)_3^{3+}$ to the excited state $[Ru(bipy)_3^{2+}]^*$. The latter subsequently emits light returning to $Ru(bipy)_3^{2+}$. This mechanism is in agreement with the observation that $Ru(bipy)_3^{2+}$ in chemiluminescent systems emits at 610 nm from the excited state $[Ru(bipy)_3^{2+}]^*$, obtained by different reactions that imply electron transfer and regeneration of the $Ru(bipy)_3^{2+}$ species.[66] The following scheme summarizes the sequence of reactions leading to the generation of chemiluminescence, as discussed above, in the presently studied experimental system 2:

$$\begin{aligned} Ru(bipy)_3^{2+} + A + Ce(IV) &\rightarrow P_1 + Ru(bipy)_3^{2+} + Ce(III) \\ P_1 &\rightarrow P_1^{\bullet} \\ P_1^{\bullet} + Ru(bipy)_3^{3+} &\rightarrow [Ru(bipy)_3^{2+}]^* + P_2 \\ [Ru(bipy)_3^{2+}]^* &\rightarrow Ru(bipy)_3^{2+} + h\nu\ (610\ nm) \end{aligned}$$

where A = analyte, P_1 and P_2 = oxidation products of the analyte.

The presently discussed signal is a novel type of second-order data that, to the best of our knowledge, has not been previously explored for achieving the second-order advantage. For each experimental sample, a series of emission spectra were recorded every 0.48 s in the range 550−650 nm, a total period of 13.92 s from the mixing of reagents, with the exciting lamp turned off. Since the spectrofluorometer is equipped with a fast-scanning monochromator set at a scan speed of 24 000 nm min^{-1}, the time required to measure a single spectrum is ~0.25 s, almost half the time between successively measured spectra. This may introduce additional complications for the subsequent data processing, since a data matrix obtained by arranging the spectra may not be strictly bilinear due to the fact that the chemiluminescence is evolving while measuring each of the intervening spectra. Notice that in the present case, the dimension with identical profiles is the spectral one, where only the ruthenium ion emits chemiluminescence. However, in the time dimension, each sample component displays a unique time evolution profile, providing the required selectivity to the analysis.

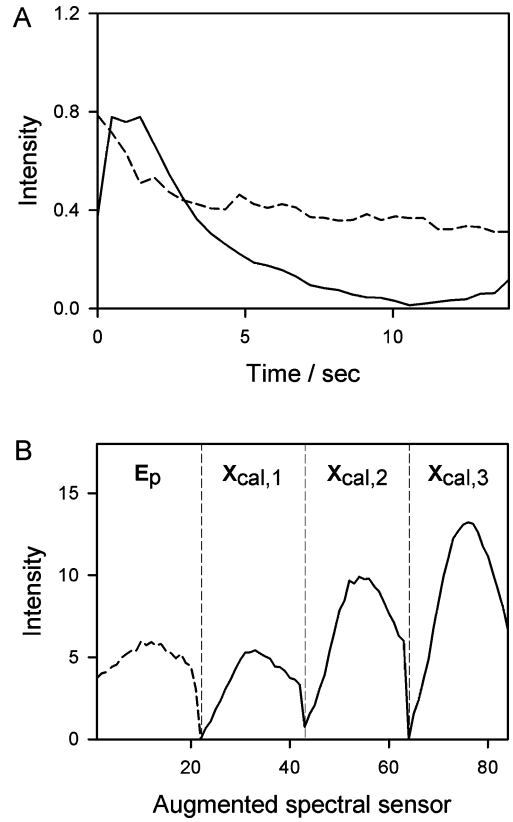

Figure 6. Profiles retrieved by U-PLS/RBL-LD (MCR-ALS version) during analysis of a typical urine sample containing ciprofloxacin: (A) time evolution profiles and (B) augmented emission spectral profiles. In both cases, the solid lines correspond to the analyte, and the dashed lines, to the interfering agent. The residual submatrix, $\mathbf{E}_p$, and the virtual calibration matrices are indicated. Vertical intensities are in arbitrary units.

As with experimental system 1, exploratory experiments showed that standard addition was required due to strong changes in the time evolution profile for the analyte when comparing a spiked urine sample and an aqueous solution of ciprofloxacin. Therefore, the same modified standard addition procedure discussed above for the previous system was employed in analyzing the present one.

Cross-validation and residual analysis allowed us to estimate that a single calibration latent variable and a single RBL-LD component were satisfactory for analyte prediction in all studied samples. When a typical urine sample was studied using the most successful U-PLS/RBL-LD method in the MCR-ALS version, satisfactory profiles were recovered in both the time and (augmented) spectral dimension. The latter ones are shown in Figure 6A and B. In this latter figure, one may appreciate the ability of the new model to separate the contribution from the urine background and that from the analyte in the residual $\mathbf{E}_p$ and in the virtual calibration matrices, as was the case for the experimental system 1.

The recovery of spectral and time profiles was of a similar quality when applying the remaining algorithms to this system, that is, MCR-ALS, PARALIND, and U-PLS/RBL-LD (PARALIND

(64) Greenway, G. M.; Dolman, S. J. L. *Analyst* **1999**, *124*, 759–762.
(65) Aly, F. A.; Al-Tamimi, S. A.; Alwarthan, A. A. *Talanta* **2001**, *53*, 885–893.
(66) García Campaña, A. M.; Baeyens, W. R. G.; Zhang, X.; Alés Gamiz, F. *Ars. Pharm.* **2001**, *42*, 81–107.

Table 3. Prediction of Ciprofloxacin in Urine Samples by Several Second-Order Models from the Time Evolution of Chemiluminescence Spectra of Ruthenium Complexes with the Sample Components[a]

	ciprofloxacin				
				U-PLS/RBL-LD	
urine	nominal	MCR/ALS	PARALIND	MCR-ALS[b]	PARALIND[b]
A	100	108	112	100	88
A	0	24	32	18	24
B	150	166	145	151	112
B	50	53	90	67	68
C	80	81	84	77	65
C	120	109	103	127	93
D	140	164	150	139	136
D	30	55	79	48	49
E	180	190	11	178	195
E	90	121	121	101	101
F	130	99	82	117	76
F	40	65	61	50	47
G	40	74	57	46	51
G	110	167	151	104	129
	RMSE[c]	26	53	10	23
	REP[d]	29	59	11	26

[a] All concentrations in milligrams per liter, referred to the original urine samples. Concentrations in the measuring cell are 10 times smaller. The letters identify the different urines employed. [b] The specific version for implementing the RBL-LD procedure is indicated. [c] RMSE = root-mean-square error in milligrams per liter. [d] REP = relative error of prediction in percent.

version). All predictive results are collected in Table 3. Overall, the results suggest than in this final experimental analysis, the new U-PLS/RBL-LD model operating in the MCR-ALS version provides the best figures of merit for a set of 14 spiked urine samples. Specifically, an RMSE value of 10 mg L^{-1} was obtained, with an associated REP of 11%. Paired *t*-statistics was also applied to the U-PLS/RBL-LD results for this set of samples (see above). The experimental value of t_{exp} was 1.7, lower than the critical $t_{crit} = 2.16$ (95% confidence level and 13 degrees of freedom), confirming that the results provided by U-PLS/RBL-LD are statistically comparable to the nominal values. A recovery test was also applied: the mean recovery for the test samples (except the blank sample no. 2 in Table 3) was 110.1%, leading to $t_{exp} = 1.8$, again lower than t_{crit} (2.18 for 12 degrees of freedom).

Regarding the comparison of the analytical results obtained with the U-PLS/RBL-LD algorithm and those achieved by MCR-ALS, it might be argued that experimental system 2 is more challenging to second-order algorithms than experimental system 1. Possible causes are (1) a larger degree of overlapping in the selective dimension (in this case, the temporal one) and (2) deviations from the bilinearity due to the finite time required to measure a spectrum during the temporal evolution of the chemiluminescence signal. The particular combination of the flexible U-PLS calibration with the specific MCR-ALS setup for the dependency-adapted RBL procedure could be better adapted to face these challenges. In any case, it may be intriguing that both MCR-ALS and U-PLS/RBL-LD achieved a similar success regarding both simulations and experimental system 1. Further work will be needed to deeply understand the behavior of specific algorithms in relation to the presently analyzed phenomena.

It may be noted that the new U-PLS/RBL-LD model has been applied in this report to several examples having a single analyte and a single interfering agent. Although the results are promising, additional work is necessary to confirm these trends in more complex samples in which additional analytes and potential interfering components occur.

CONCLUSIONS

Simulations and experiments involving second-order data in the presence of identical profiles in one data dimension show that a new model, which couples unfolded partial least squares with residual bilinearization for linear dependency, is able to achieve the second-order advantage. The success in reaching the latter advantage and quantitating the analyte is comparable to a previously tested multivariate curve resolution/alternating least-squares model.

ACKNOWLEDGMENT

Universidad Nacional de Rosario, CONICET (Consejo Nacional de Investigaciones Científicas y Técnicas, Project No. PIP 1950), and ANPCyT (Agencia Nacional de Promoción Científica y Tecnológica, Project No. PICT04-25825) are gratefully acknowledged for financial support. V.A.L. thanks CONICET for a fellowship.

Received for review February 16, 2010. Accepted April 23, 2010.

AC100424D